# CHARACTERIZATION AND HIGH-THROUGHPUT MICROFLUIDIC APPLICATIONS OF AN OBSTRUCTED-CHANNEL FLOW CLASS

**Kamen N. Beronov**, **Nagihan Özyilmaz**
Lehrstuhl für Strömungsmechanik, Universität Erlangen-Nürnberg
Cauerstr. 4, D-91058 Erlangen, Germany
{kberonov,noezyilm}@lstm.uni-erlangen.de

## ABSTRACT

Microfluidic devices have been so far limited to creeping flow regimes, with various kinds of forcing, of mixing, of flow patterns, but with inadvertently low flow rates acceptable for miniaturized medical diagnostics but not for even small-batch synthesis. The latter and related applications began only very recently to attract industrial attention, bringing microfluidic design tools into difficulties as these are now confronted with chaotic and low-Reynolds-number turbulent flows. The present investigation focuses on a newly introduced, generic kind of mixing elements in microchannels and pressure driven flows in a Reynolds numbers range $500 < Re < 2000$. It overcomes the mentioned limitations by resorting to direct 3D simulations and appropriate, highly efficient numerics. The results show clearly that turbulence can be generated, maintained at essentially linear cost, and controlled by suitable arrangements of large obstructions across the mean flow in micro channels. Genuine 3D turbulence can thus be maintained at Reynolds numbers several times lower than the critical $Re_c$ of straight channels.

## INTRODUCTION

Flows through channels with profiled walls or roughness elements have been studied experimentally and numerically in various contexts, mainly in mass and heat transfer contexts, but also in turbulence generation, mixing enhancement, etc. The design and control of these flow sections requires the examination of many parameters. Here we focus on the selection of roughness element profile with specific emphasis on vortex stretching.

Most often, the converging sections have simple square cross-sections. The simple geometry considered here deviates from that standard and allows a first exploration of the possibilities to induce and control the three-dimensionality of mixing channel flows at lower energy input levels as before.

The present paper investigates data from three detailed numerical simulations on such geometries. It adresses only the mean flow and vorticity statistics and structures with respect to aspect ratio. This is sufficient to show qualitatively the potential for enhancement of passive flow control through simple design optimization of obstructed channel geometry.

## SIMULATION SET-UP

Large eddy simulations (LES) using the standard Smagorinsky model with Smagorinsky constant set to $C_s = 0.01$ were carried out. A standard lattice Boltzmann method (LBM) with BGK relaxation and D3Q19 lattice model was used as solver. The flows are driven by a constant "pressure force" in the mean flow direction $x$ and assumed spatially periodic in $x$ and in the spanwise direction $z$. The channel height in the $y$ direction depends on the location $x$. Two channel geometries vary in streamwise direction, in a single way that can be inferred from Figure 1, having 45° contractions of aspect ratio $\alpha = 2$ and $\alpha = 4$ respectively. Turbulence is excited only during an initial period, by enforcing streamwise vortical flow structures without added net impulse.

The simulations were found *a posteriori* to be effectively model-free (direct numerical simulations), since the ratio between the turbulent and Newtonian viscosity is $4 \times 10^{-5}$ in the $\alpha = 2$ run and $1.9 \times 10^{-5}$ in the $\alpha = 4$ run. The mesh resolution was $256 \times 96 \times 64$ in all runs. The full height of the narrow channel in lattice units (LBM use equal, constant mesh steps in all directions) was 48 for $\alpha = 2$ and 24 for $\alpha = 4$. The driving pressure drop and the amplitude of the initial streamwise vortices were kept the same, so that the resulting mean flow Reynolds number depend only on the contraction ratio. Since the flow resistance of a narrower channel is larger, they different: $Re_m = 2150$ for $\alpha = 2$ and $Re_m = 600$ for $\alpha = 4$. Here, $Re_m$ is calculated from the streamwise mean velocity (averaged in time as well as in the streamwise and spanwise directions) and the full height of the narrow channel part.

In order to induce turbulent structures, one streamwise vortex was enforced by a time-independent bodyforce, centered in the middle of the narrow channel for both aspect ratios. In a further set of simulations with $\alpha = 2$, the position was shifted towards the wall. These two positionings will be referred to as "centered forcing" and "top forcing" hereafter. After reaching a statistically steady state of the flow, this kind of forcing was switched of and the run was continued. It will be named "decaying," although the streamwise, uniform "pressure drop" was maintained unchanged.

Two ways of averaging were applied: For a characterisation of the mean velocity profile in the whole channel, quantities were averaged in time and in the spanwise direction only. For studies in the narrow channel part, they were also averaged in streamwise direction over the $x$-length of that channel section.

## FORCED FLOW

We consider first the flow statistics obtained under constant "vortex enforcement," as opposed to "decaying" vorticity. The results provide a basis for comparison and an illustration of the effect of Reynolds number in relation with the choice of geometry.

### Mean flow

Figure 2 shows the time-averaged streamwise velocity component for the simulated geometries. (The vertical axis

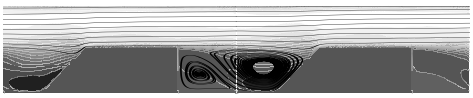

(a)

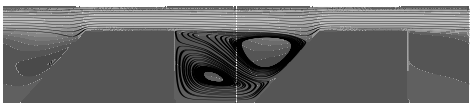

(b)

Figure 1: a) Contours of streamwise velocity–Aspect 2, b) Contours of streamwise velocity–Aspect 4.

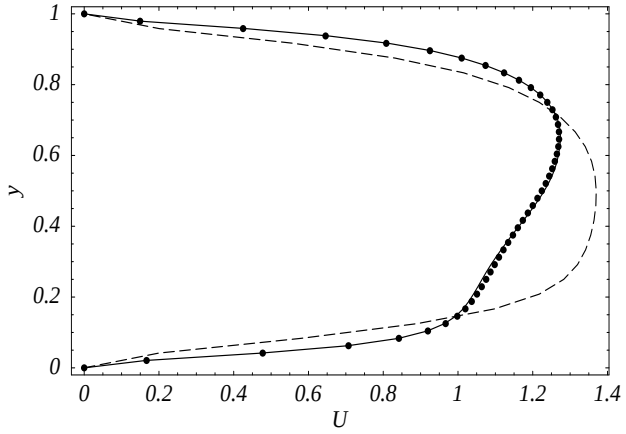


Figure 2: Time-averaged streamwise velocity, averaged in streamwise and spanwise directions over the narrow channel; points: $\alpha = 2$ with "top" forcing, solid line: $\alpha = 2$ with "centered" forcing, dashed line: $\alpha = 4$.

is normalized by the full height of the narrow channel. The velocity profiles were normalized by the bulk velocity in the narrow channel section.) A difference in Reynolds numbers is clearly inferred from these data: While for $\alpha = 4$ the profile is nearly parabolic and thus of "laminar type," in the $\alpha = 2$ case the velocity closer to the upper wall is higher than at corresponding locations closer to the lower wall, suggesting strong inertial effects.

The influence of the position of the "forcing" on the mean velocities is negligible: the two profiles for $\alpha = 2$ effectively overlap in Figure 2. Both in the "narrow" and the "wide" sections of the channel, asymmetry is not observable in the (lower Reynolds number) case $\alpha = 4$.

An important flow property is illustrated by Figure 1. (There, lighter grey indicates a higher value of velocity.) In the case of higher Reynolds number, a nearly "streamwise" vorticity enhancement, as expected due to the contraction, is clearly observable only close to the lower edge of the narrow channel. In the lower $Re_m$ case, however, this effect of vorticity enhancement spreads over the whole cross section of the narrow channel. This shows a way of passive control — through the design of the contraction aspect ratio — to influence the location and strength of vortex structures.

Turning to the spanwise (2D) vortices seen in Figure 1, the slope of the cross section of the vortex structure closer to the lower end of the narrow channel is about the same across all cases simulated, i.e. the data suggest that the vortex structure (induced by the same kind of "vortex forcing") is approximately *independent* of the geometry.

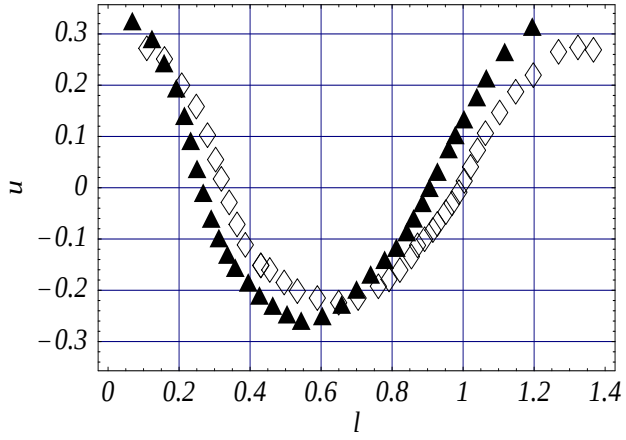


(a)

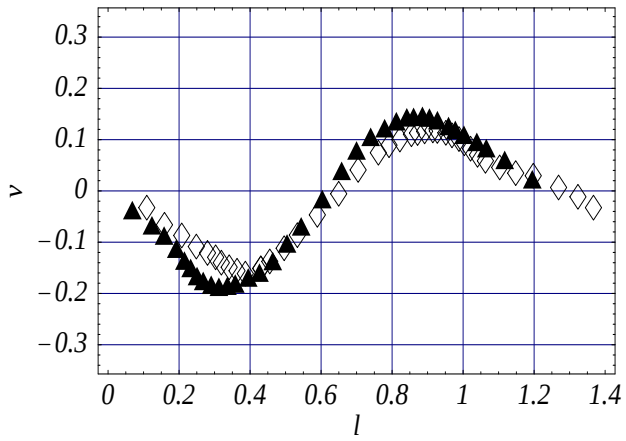


(b)

Figure 3: a) Characterisation of the upper vortex in Figure 1(a) with respect to streamwise velocity component, b) Characterisation of the upper vortex in Figure 1(a) with respect to normal velocity component.

To verify the latter hypothesis, the position of the center of this vortex and the position of the corresponding stagnation point were evaluated. At a vertical position corresponding to half the distance between the center of the vortex and the stagnation point, streamlines were traced as demostrated in Figure 3. They show the magnitude of the streamwise and the normal velocity components on the reference vortex. It can be argued that a good agreement in the spanwise (primary) vortex structure exists between different geometries and Reynolds numbers. It is noted that the height of the vortex seen in Figure 1 is the same for each aspect ratio to within 3%.

#### Stability of streamwise vortices

Figure 4 shows instantaneous structures of streamwise velocity and vorticity components at three subsequent time steps for $\alpha = 2$ with "centered" forcing. Isolines represent velocity and shading represents vorticity. Contours are shown on $y - z$ plane normal to the mean flow direction. There is a marked change in time, both in velocity and in vorticity structures. Similarly, Figure 5 shows instantaneous structures at three subsequent time steps for $\alpha = 4$. More detailed observations of this kind, as well as spectral data provide solid ground to state that the observed flows are turbulent, 3D and strongly mixing, even at the lowest $Re_m$

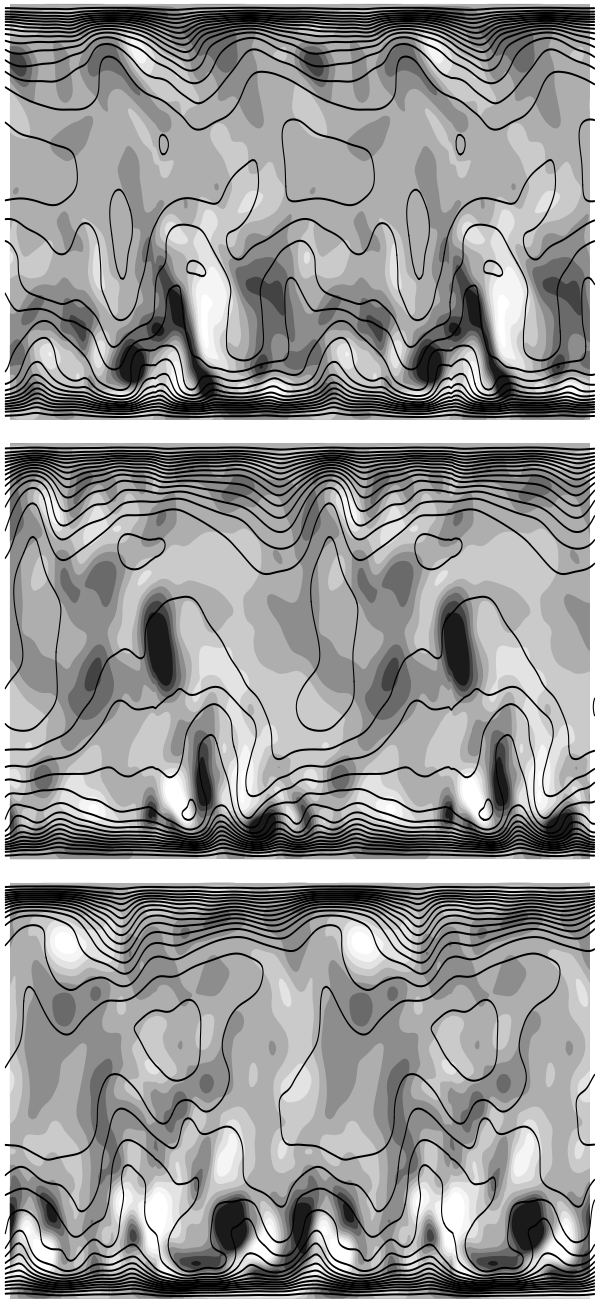

Figure 4: Instantaneous streamwise velocity and vorticity contours of aspect 2 with "centered" forcing at three subsequent time steps.

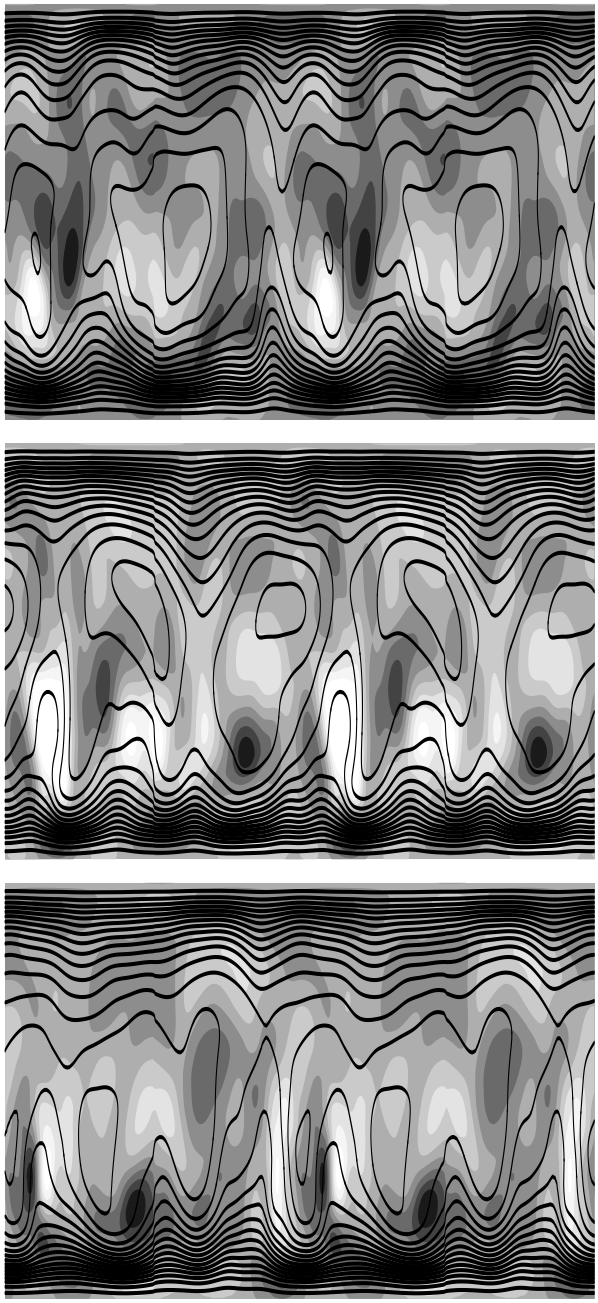

Figure 5: Instantaneous streamwise velocity and vorticity contours of aspect 4 with "centered" forcing at three subsequent time steps.

simulated. The latter is several times lower than the critical Reynolds number for plane channels. Thus, the introduction of vortical forcing and of voriticity-enhancing wall profiles allows the production of sustained turbulence at much lower flow rates and pressure drops in comparison to what can be achieved (through spontaneous or triggered instabilities) in simple plane channels. The general observation is not entirely new, as pointed out e.g. by Lammers and Jovanovic (2005), but the use of vortex stretching geometries allows much lower turbulent Reynolds numbers than simple rectangular obstacles.

Figure 6 and Figure 7 show instantaneous structures of streamwise velocity at two different time steps. The shown velocities were processed as follows: The instantaneous raw data were normalized in each layer parallel to streamwise direction by the maximum velocity in the corresponding layer. Then the obtained velocities processed further according to the following formula, where U denotes the streamwise velocity normalized by the maximum velocity: $\log(1-U^2/(1.2))$.

## VORTEX DECAY

Having seen the effect of the imposed streamwise vortex, the simulations were continued without this force for two flow-through times and the quantities were compared with corresponding data from the simulations with vortex forcing. This change caused a slight decrease in the magnitude of the velocity components but the dominant structures survived. The time averaged mean streamwise velocity profile did not change dramatically. The magnitude of instantaneous streamwise vorticity component at three distinct time

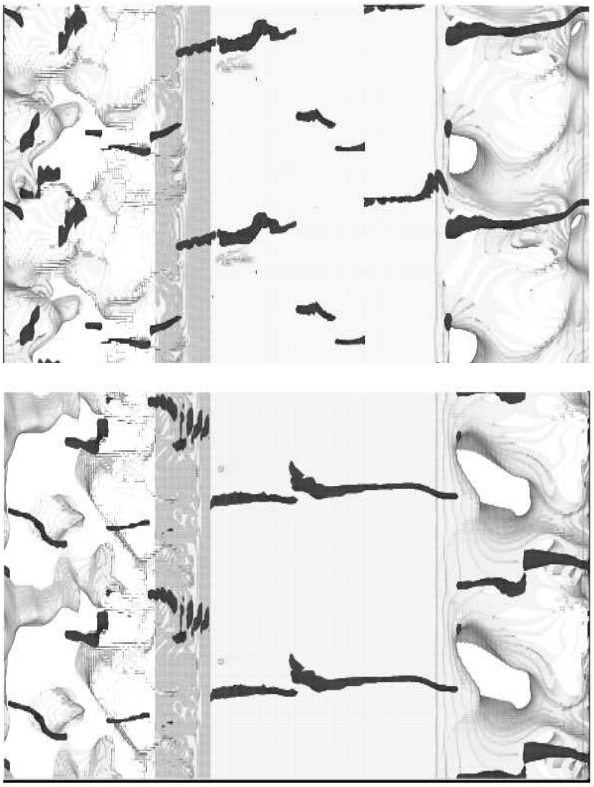

Figure 6: Instantaneous structures of streamwise velocity at two different time steps.

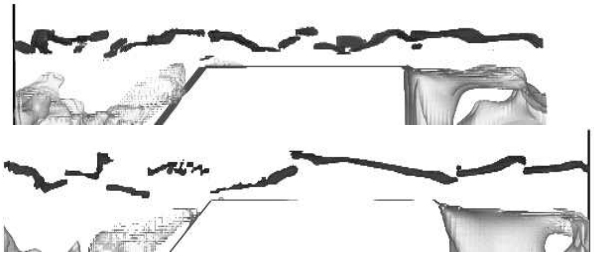

Figure 7: Same as 6, but side view.

steps.

The vortex enhancement due to strong accelaration causes streamwise structures in both cases. In particular, the turbulence observed for $\alpha = 4$ is maintained at a Reynolds number several times smaller than the critical value below which only laminar flow can be obtained in a plane channel. The time for which the time-averaged streamwise structures survive after switching off the corresponding forcing in this direction is examined: the decay of the magnitude of the streamwise vorticity is very slow in both cases. Slow streaks are found inside regions of intense vorticity and fast jets between them. The influence of the position of the initially introduced streamwise vorticity is found to be irrelevant to the locations of the large-scale structures found later in the flow.

It is found that only in the higher aspect ratio case, a *time-independent coherent* flow structure could be observed even after switching off the vortex forcing. This means that under a sufficiently strong contraction and at sufficiently high Reynolds numbers, an initially superposed streamwise vortices can survive alone due to the suitable passive control through vortex stretching.

## MICROFLUIDIC APPLICATIONS

The term "high-throughput microfluidics" is usually used to describe lab-on-a-chip designs which permit the (relatively) fast processing of a large number of (very small, typically of nano-liter individual volume) samples. In the last two years, the same name or sometimes the notion of "high-pressure microfluidics" have come to be used in conjunction with novel designs of microfluidic devices, whose main purpose is to increase the throughput in terms of volume flow while keeping the advantages of microfluidic components, such as best control of process parameters (temperature, volume flow rate), scalability, etc. In the process of development of such devices — in particular of passive and active micromixers meant for high flow rate (as compared to "standard" lab-on-a-chip) continuous or batch processing in the chemical and pharmaceutical industry — it was recognized that the usual design tools based on steady laminar flow (and most often explicitly on creeping flow) assumptions fail when confronted with results from verification experiments. The need for detailed time-dependent simulations of flows in microchannels (mixers as described above, direct injection of engine fuel, etc.) has now been recognized.

The present work provides a set of reference results, showing the importance of time-dependence and three-dimensionality in the design of such high-throughput microfluidic devices, even if the effect of transient flow actuation is neglected. The results confirm the expectation, that with suitable modifications of channel design — in particular by using asymmetric "roughness elements" placed in sufficient number along one or more walls of such channels — it is possible to induce, enhance and even to sustain indefinitely truely turbulent flows, characterized by essentially 3D mixing. A very important observation is that these positive features (from the point of view of most microfluidic design tasks) do not incur undue increase in pressure drop — a decisive advantage compared with common "porous media" based designs of micromixer components. Even in the presence of sustained streamwise vortices, the overal pressure drop remains very close to that of plane channels of corresponding dimension. The flow actuation must be carefully selected, however, so that the effective Reynolds number remains below 2000. This not only assures a "linear" pressure loss, but also optimal mixing since it means that the vortical structures have cross sections comparable to those of the whole channel and not to that of a very thin boundary layer.

Future investigations would reveal optimal shapes and spacings for the kind of roughness elements considered here and other related geometries. The qualitative results presented here can already be tranfered, that is, anticipated with certainty, for a wide class of microchannel geometries, including circular and square cross-sections.

## REFERENCES


Eloranta, H., Parssinen, T., Saarenrinne P., Poranen J., and Sekki, H., 2006, "On the fluid-structure interaction of a splitter plate: vibration models and Reynolds number effects," *Experiments in fluids*, Vol. 41, pp.67-77.

Murphy, H.D., Chambers, F.W., and McEligot, D.M., 1983, "Laterally converging flow. Part 1. Mean flow," *Journal of fluid mechanics*, Vol. 127, pp.379-401.

Nasr, A., and Lai, J.C.S., "A turbulent plane offset jet with small offset ratio," *Experiments in fluids*, Vol. 24, pp.47-57.

White, F., 2003, "Fluid Mechanics", McGraw Hill.